RESEARCH LETTER

### γδ T Cells Control Gut Pathology in a Chronic Inflammatory Model of Colorectal Cancer

Gut γδ T cells are intraepithelial lymphocytes with reported roles in maintaining the gut barrier against infection and epithelial stress.[1,2] In addition, absence of γδ T cells leads to faster polyp formation in an inflammation unassociated model of colorectal cancer (CRC) and γδ T cells reportedly showed antitumor activity in the context of human CRC.[3,4] Patients with inflammatory bowel disease with early CRC have heightened risk for surgery with a different evolutionary history and genomic characteristics compared with sporadic CRC.[5-7] To investigate the unknown role of γδ T cells in inflammatory bowel disease–associated CRC, we used a new murine model (chronic AOM-DSS).

We observed diminishing γδ T cells in colonic intraepithelial lymphocytes of AOM-DSS mice, associated with reduced trends in epithelial-anchorage-molecules and TCR γδ genes (Supplementary Figure 1). To validate the pathologic impact of γδ T cells' loss, we investigated polyp formation in the presence or not of γδ T cells (Figure 1A and B and Supplementary Figure 2A-F). Interestingly, we observed a body weight difference in this model only after the 2nd cycle of DSS (Figure 1A), in contrast to acute DSS colitis.[1] At the termination (Day 58), gross pathologic parameters of colon were significantly increased in TCRδ-/- mice (Supplementary Figure 2B). TCRδ-/- mice with AOM-DSS showed increased histologic inflammation and increased polyp formation (Figure 1B and Supplementary Figure 2C). Polyps in the distal colon were limited to small regions in WT mice but were multifocal to widespread in TCRδ-/- mice (Supplementary Figure 2D and E). Quantification with Ki67 and Bcl2 revealed that polyps in TCRδ-/- mice were more prevalent in the distal colon compared with the proximal colon with increased proliferation and anti-apoptosis (Supplementary Figure 2F).
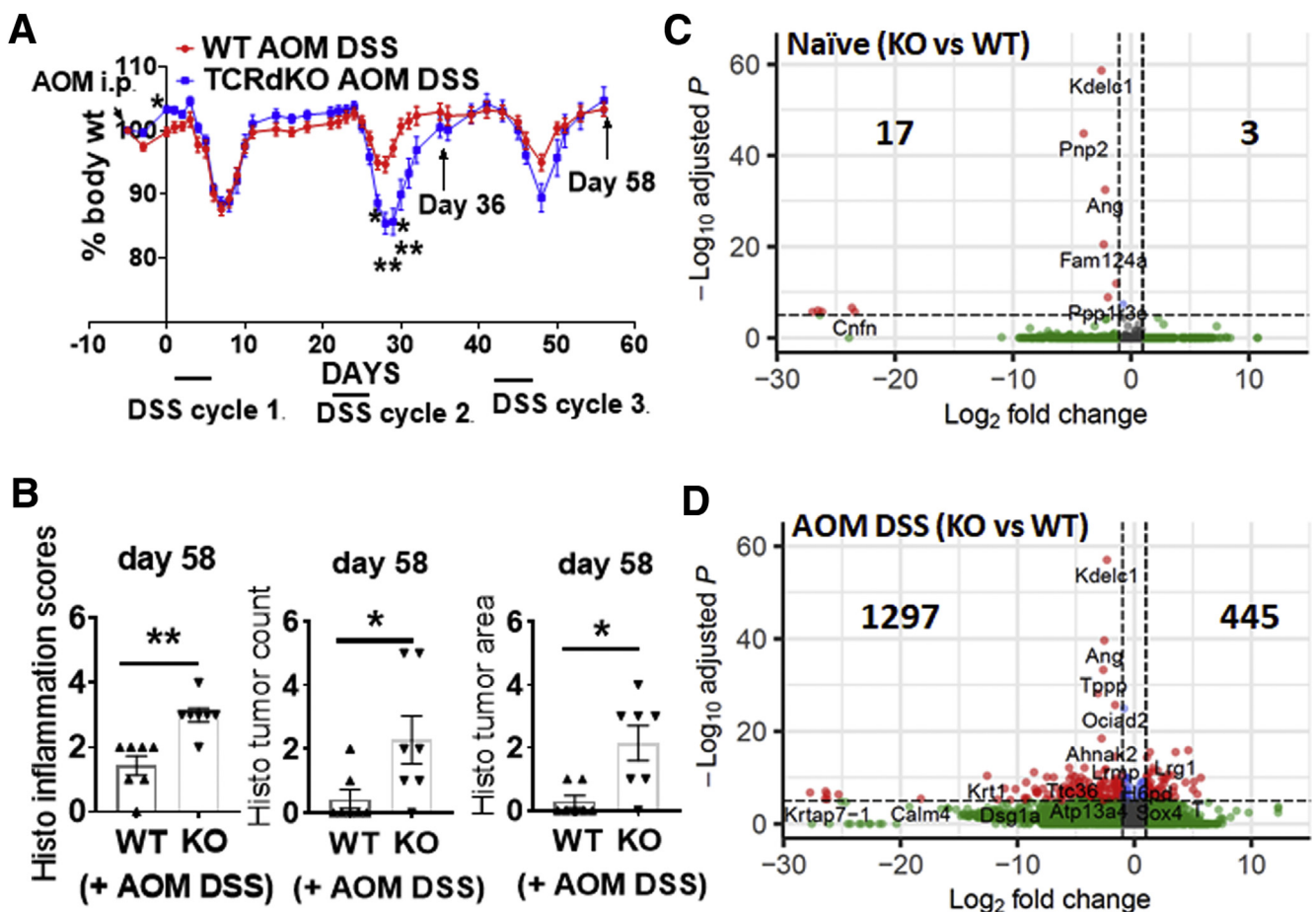
Figure 1. Lack of γδ T cells enhances gut pathology and tumorigenesis in a chronic AOM-DSS model. (A) Representative comparative body weight loss curve from 2 independent experiments (n = 30/strain). (B) Day 58 histologic scores (1-cm colon) from animals as shown in Supplementary Figure 2B. (C, D) Volcano plots showing the DEGs comparing KO versus WT in each model. Cutoffs: fold change ≥2; adjusted $P \leq .05$. KO, knock-out.
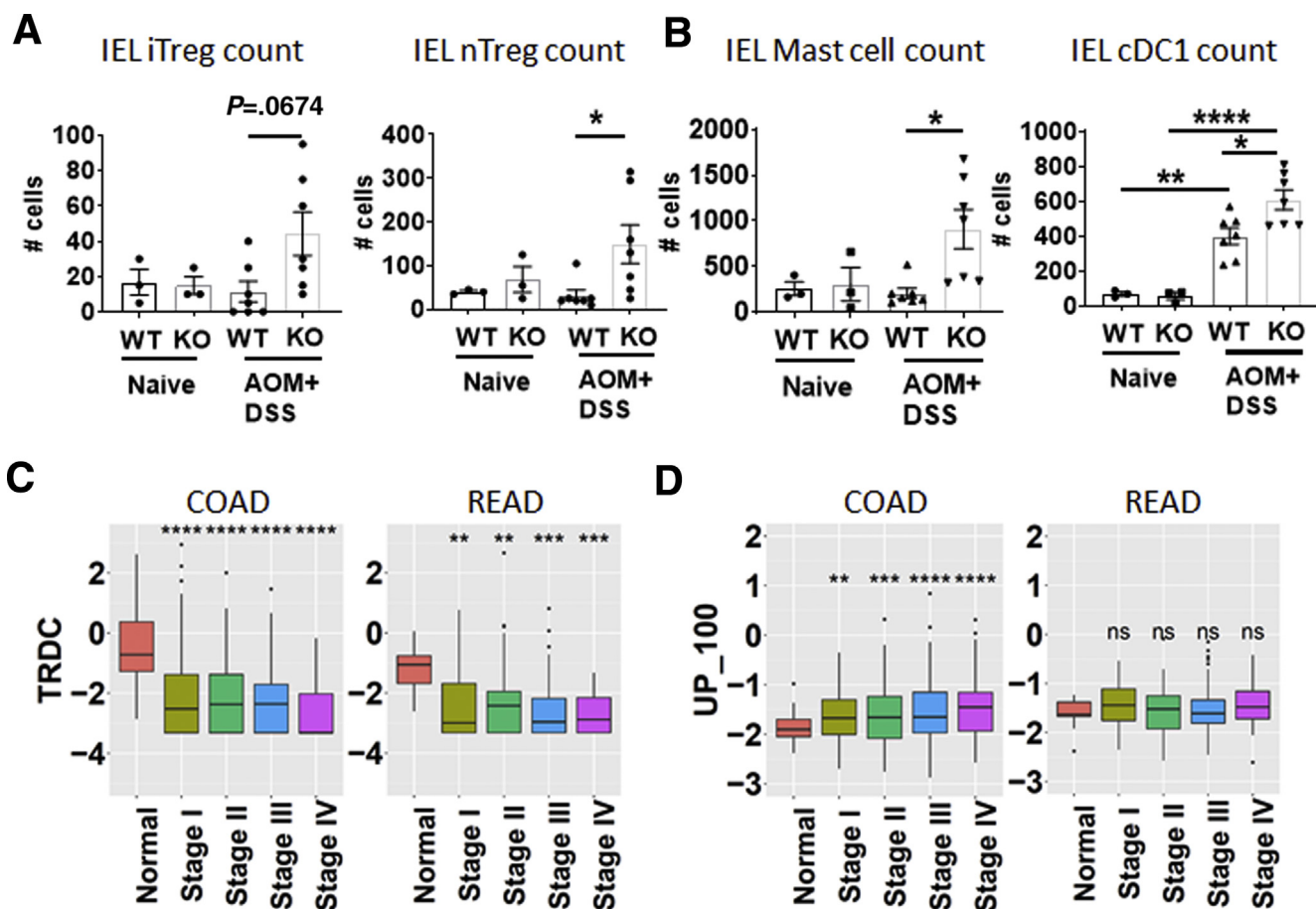
Figure 2. γδ **T cells control immunoregulatory phenotype in IEL and correlate negatively in COAD.** (A) Cell numbers of Tregs in IEL. (B) Cell numbers for Mast cells (*left panel*, live CD45+Epcam-CD3-B220-ckit+) and cDC1s (*right panel*, live CD45+Epcam-CD3-CD19-MHCII+F4/80-CD11c+CD11b-CD103+). (C) Expression of TRDC at different stages of COAD/READ tumors and related normal. (D) Median expression of top 100 upregulated genes (KO vs WT in AOM+DSS) in the same dataset. IEL, intraepithelial lymphocytes; KO, knock-out; ns, not significant.

Thus, absence of γδ T cells chronically induced early polyp formation qualitatively and quantitatively.

To identify the early molecular events underlying gut pathology mediated by loss of γδ T cells, we focused on an early time point after the 2nd cycle of DSS. Polyps were not grossly observed in the colon of WT or TCRδ-/- mice but were observed microscopically in the distal colon of TCRδ-/- mice (Supplementary Figure 2G). Because polyp initiates in the distal region, this location provided opportunity to observe differential gene expression (RNAseq) without the bias of number and shape of polyps. Principal component analysis revealed well-separated clusters of AOM-DSS treatment from respective naive groups and WT cluster was separated from TCR δ-/- cluster within

AOM-DSS treatment (Supplementary Figure 2H).

We identified a massive transcriptional reprogramming with 445 upregulated differentially expressed genes (DEGs) and 1297 downregulated DEGs in AOM-DSS treatment groups comparing TCR δ-/- mice versus WT counterpart (Figure 1C and D). The number of DEGs in untreated naive mice was much lower emphasizing the requirement of tissue insult to reveal γδ T cells' functions. Pathway enrichment analysis on DEGs (CPDB, Supplementary Figure 3A and B) has revealed upregulation of several signaling pathways including destructive structural pathways and while some beneficial structural pathways were downregulated. Similar results were obtained using DAVID pathway analysis (data not shown). In detailed

analysis, inflammation and inflammation-associated oncogenes were upregulated, whereas some anti-inflammatory, antiangiogenesis, gut homeostasis, structural integrity, and tumor suppression genes were significantly downregulated (Supplementary Figure 3C-M). Overall, we identified a profound γδ T cell–dependent transcriptional reprograming of gut tissues that emerges early and affects broad cellular functions.

We wondered whether γδ T cells' presence could delay the appearance of an immunoregulatory environment, a hallmark of protumor condition. We evaluated several cells and observed augmentation of Helios+Foxp3+ natural Tregs (nTregs) and 2 myeloid cell types: mast cells and conventional dendritic cell 1 (cDC1), known to induce/maintain/associate with

CD4+Tregs.[8-10] nTregs were augmented in the intraepithelial lymphocytes in contrast to the LP fraction of TCR δ-/- mice on Day 58 following AOM-DSS treatment (Supplementary Figure 4A and B and Figure 2A and B).

Analyzing transcriptomic data from CRC tumor patients, we found that TCR delta chain constant region (TRDC) gene expression was consistently lost in early to late stages of tumors (along with TRGC and known epithelial-anchorage-molecules but reverse trend in FOXP3) (Figure 2C and Supplementary Figure 4C-G). Interestingly, the median expression of the top 100 upregulated genes in the absence of γδ T cells (TCRδ-/- vs WT, AOM-DSS treatment) was robustly upregulated at different stages of colon (but not rectal) adenocarcinoma (Figure 2D). Therefore, loss of γδ T cells and the associated upregulation of the gene signature observed in early tumorigenesis in our mouse model are also found in cancer patient samples.

Our data reveal a profound protective feature of gut γδ T cells in a relevant chronic gut pathology model that was confirmed to be present in CRC patient samples. These results shed light on the physiologic relevance of these cells in intestinal epithelial barrier integrity, and as critical sentinels against early tumorigenesis. Further investigations involving targeted approaches for differentially expressed candidate genes identified in our datasets, in the context of the murine model, would be helpful. Manipulation of these cells may confer therapeutic benefits in CRC, and their broader spectrum of applications warrant further investigation.

SURYASARATHI DASGUPTA[1,a]
HONG LIU[2,3,a]
BRANDI BAILEY[1]
COREY WYRICK[1]
JESSICA GRIEVES[4,5]
CHRIS DEBOEVER[6]
CRAIG MURPHY[1,7]
BENJAMIN FAUSTIN[1,8,9]
[1]GI Immunology Research, GI DDU, Takeda California Inc, San Diego, California
[2]Immune-Oncology DDU, Takeda Pharmaceuticals, Cambridge, Massachusetts
[3]Translational Research, Checkmate Pharmaceuticals, Cambridge, Massachusetts
[4]Global DSRE, Takeda California Inc, San Diego, California
[5]Ionis Pharmaceuticals, Carlsbad, California
[6]Computational Biology, Takeda California Inc, San Diego, California
[7]Immunology Translational Science and Medicine, Janssen Research and Development, San Diego, California
[8]ImmunoConcEpt Laboratory, CNRS UMR 5164, Bordeaux University, Bordeaux, France; and
[9]Immunology Discovery, Janssen Research and Development, San Diego, California
Address correspondence to: Suryasarathi Dasgupta, Takeda Pharmaceuticals USA Inc, 9625 Towne Center Drive, San Diego, California 92121. e-mail: suryasarathi.dasgupta@takeda.com or Benjamin Faustin, 520 Via De La Valle, Unit C, Solana Beach, California 92075. e-mail: benfaustin@gmail.com.

References

1. Kober OI, et al. Am J Physiol Gastrointest Liver Physiol 2014; 306:G582–593.
2. Lee JS, et al. Immunity 2015; 43:727–738.
3. Matsuda S, et al. Jpn J Cancer Res 2001;92:880–885.
4. Mikulak J, et al. JCI Insight 2019; 4:e125884.
5. Kim ER, et al. World J Gastroenterol 2014;20:9872–9881.
6. Baker AM, et al. Gut 2019; 68:985–995.
7. Kameyama H, et al. World J Surg Oncol 2018;16:121.
8. Eller K, et al. J Immunol 2011; 186:83–91.
9. Yang Z, et al. PLoS One 2010;5: e8922.
10. Maldonado RA, et al. Adv Immunol 2010;108:111–165.

Supplementary Material and Methods

Mice female C57Bl/6J mice, WT (000664) or TCRδ-/- (002120), were bred in Jackson Laboratories (Bar Harbor, ME) and age matched (6–8 weeks old) batches were transferred together and maintained under similar specific-pathogen free conditions for at least 2 weeks before starting any experiment at Takeda California's animal facility.

AOM-DSS Model

Post 5 days of azoxymethane (intraperitoneally 12 mg/kg AOM, Sigma Aldrich, St. Louis, MO) administration, mice were fed with water containing 3% DSS for 3 cycles of 5 days. Four independent experiments were performed with WT mice, among which the last 2 were comparing WT with TCRδ-/- strains. All mice were sacrificed at indicated time points using CO_2-based euthanasia as per our animal facility regulations.

Histology

Colon tissue was fixed overnight and embedded in paraffin blocks, followed by histostaining (HistoTox Labs, Boulder, CO). Slides were scanned using an Aperio AT2 whole slide scanner and blind scored. For inflammation, the following scoring system was used: 0 = normal, 1 = minimal (<10% of mucosa), 2 = mild (11%–25% of mucosa), 3 = moderate (26%–50% of mucosa with minimal to mild expansion of crypts ± minimal crypt effacement), 4 = marked (51%–75% of mucosa with mild to moderate expansion of and effacement of crypts), and 5 = severe (>75% of mucosa with extensive crypt effacement). For tumor percentage area, the following scoring system was used: 0 = no tumors, 1 = <10% of mucosal surface expanded by tumors, 2 = 11%–25% of mucosal surface expanded by tumors, 3 = 26%–50% of mucosal surface expanded by tumors, 4 = 51%–75% of mucosal surface expanded by tumors, and 5 = >75% of mucosal surface expanded by tumors.

For immunohistochemistry staining in FFPE mouse colon swiss rolls, staining was conducted on a Leica Bond RXm using standard chromogenic methods. For antigen retrieval (HIER), slides were heated in either a pH6 citrate-based buffer (for Bcl-2, Boster Biological Technology, A00040-2), or a pH9 EDTA-based buffer (for Ki-67, Cell Signaling Technology, 12202) for 25 minutes at 94°C, followed by a 30-minute (Ki-67, 1:100) or 45-minute (Bcl-2, 1:80) antibody incubation. Slides were annotated to delineate regions of interest identified as regions associated with proximal and distal colon mucosa; proximal colon was defined as colonic tissue exhibiting mucosal folds.

Using regions of interest, an algorithm was applied to the stained samples using Visiopharm (VIS) image analysis software.

Isolation of Colonic Cells and Flow Cytometry

Cell isolation and staining were performed using protocol as previously published by our group.[1] Single cell suspensions from intraepithelial lymphocytes and LP were prestained with Zombie Aqua (Biolegend, San Diego, CA) fixable viability kit and then labelled with a cocktail of fluorochrome conjugated antibodies against surface antigens purchased from BD Biosciences (San Jose, CA), Biolegend (San Diego, CA), or Fisher/eBioscience (San Diego, CA). Cells were fixed with IC Fix (Fisher/eBioscience) before acquisition in flow cytometry. Alternately for T-cell transcription factors and cytokines, single cell suspensions from intraepithelial lymphocytes and LP suspended in RPMI1640 + 10% fetal bovine serum + Pen/Strep/Glutamine and incubated with Lymphocyte Activation Cocktail (5 ng/mL PMA + 0.5 μg/mL ionomycin + Golgiplug, BD Biosciences) for 4 hours at 37°C. Cells were washed and resuspended in Fix/Perm Buffer (Fisher/eBioscience) overnight followed by staining. Fixed volume of cell suspensions were acquired (100 μL) from fixed volume of original suspension (500 μL). Cells were acquired using the 18-color BD LSRFortessa X-20 (San Jose, CA) and analyzed with FlowJO software (Ashland, Oregon).

Gene Expression Experiments and Analysis

Snap frozen terminal 1-cm distal colon tissue samples, n = 3 for each group (Figure 1 E-G, Supplementary Figure 3) and n = 6 for naive, n = 2 for day 32, and n = 4 for day 55 (Supplementary Figure 1B), were sent to Q2 solutions (Morrisville, NC) for bulk RNA sequencing. Same isolated mRNA was used for nanostring and TCR-sequencing. Total RNA was prepared with the miRNeasy Mini method (Qiagen). The quantity and integrity of mRNA were measured using the 2100 Bioanalyzer system with Nano chips (Agilent Technologies).

Bulk RNA-seq

Fastq files generated by Q2 solutions were processed in OmicSoft Array Studio (V10.1) using RNA-seq analysis pipeline, which includes QC, sequence reads mapping, and gene count/FPKM quantification. DESeq General Linear Model was constructed to compare samples in knockout versus WT for each model (naive, AOM-DSS). DEG was defined as gene with fold change ≥2 and adjusted P value (Benjamini–Hochberg false discovery rate) ≤ .05. Pathway enrichment analysis for DEGs were performed in both CPDB (http://cpdb.molgen.mpg.de/) and DAVID (https://david.ncifcrf.gov/). Volcano plots were generated using the Enhanced Volcano package (version 1.0.1).

Nanostring Analysis

Samples were adjusted to 20 ng/μL for nanoString analysis. Samples were processed via custom nanoString mouse gene expression panel and data generated via nanoString nSolver software. Select genes were normalized to b-actin and relative expression reported.

TCR-Sequencing Analysis

Sequencing of gamma-delta TCR CDR3 was performed by iRepertoire (Huntsville, AL). CDR3 quantification and gene usage was performed by iRepertoire. Differential gene usage

was identified by comparing the fraction of CDR3 reads per sample that contained a particular gene between naive and AOM chronic DSS day 32 or day 55 samples. Two of 4 samples from AOM chronic DSS day 55 mice failed TCR sequencing (less than 20 reads obtained) and are not included in the analysis.

Patient Data

COAD (colon adenocarcinoma) and READ (rectum adenocarcinoma) RNA-seq data were from TCGA (https://www.cancer.gov/about-nci/organization/ccg/research/structural-genomics/tcga).

Statistical Analysis

In Figure 1, plot A shows the mean ± SEM for percent body weight for each strain at each time. A mixed effect analysis was used with animal as the random effect and time, strain, and time × strain as fixed effects. Fixed effects of time and time × strain were found to be significant overall ($P <$ .0001 for both), whereas strain alone was not. The significant differences in % body weight between the 2 strains, using Sidak multiple comparisons test (GraphPad Prism software **$P <$ .01; *$P <$ .05), are indicated with asterisk. For plots B, C, and D, error bars in the bar graphs signify mean ± SEM for each bar and each dot represents individual animal. Statistical analysis using nonparametric Mann-Whitney test was performed.

In Figure 2, for animal experiments (B-D), error bars signify mean ± SEM for each bar and each dot represents an individual animal. Statistical analysis using 1-way analysis of variance with Tukey multiple comparison was performed. For patient data analysis (E and F), Student t test was conducted. ****$P <$ .0001; ***$P <$ .001; **$P <$ .01; *$P <$ .05.
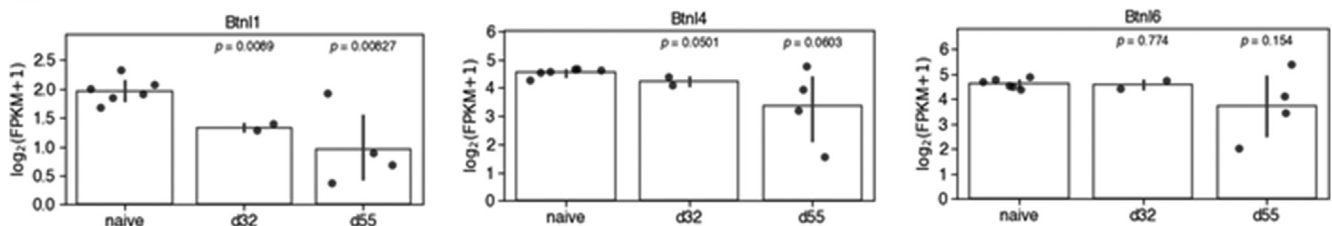
Reference

1. Liu H, et al. BMC Immunol 2019; 20:42.

A
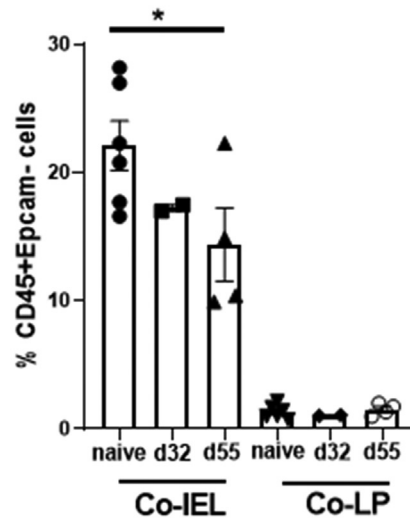
B

C
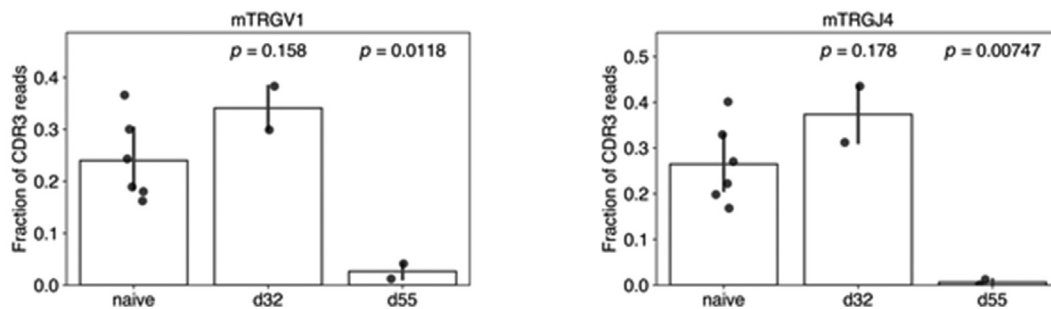

Supplementary Figure 1. Reduction of $\gamma\delta$ T cell–associated parameters in colonic IEL in AOM DSS model. WT B6 female mice were treated with AOM (12 mg/kg, 2 days before 1st cycle of DSS) and 3% DSS (3 cycles). Mice were sacrificed on days 32 and 55 postinitiation of DSS. Colonic IEL and LP fractions (entire colon except last 1 cm) were analyzed by Flow cytometry for $\gamma\delta$ T cells (TCR delta+CD3+ in CD45+Epcam- live cells) (*A*). RNA was isolated from the last 1 cm of each colon and bulk RNA sequencing and TCR sequencing were performed. Gene expression of *Btnl* genes related to $\gamma\delta$ T cells biology in murine intestine (*B*). Usage for γ TCR chains was measured by TCR CD3 sequencing (*C*). Mean ± SEM, each dot represents an individual animal. Differential expression of TCR chain usage was assessed using an unpaired Student *t* test between naive versus day 32 or day 55 samples. *$P < .05$. IEL, intraepithelial lymphocytes.
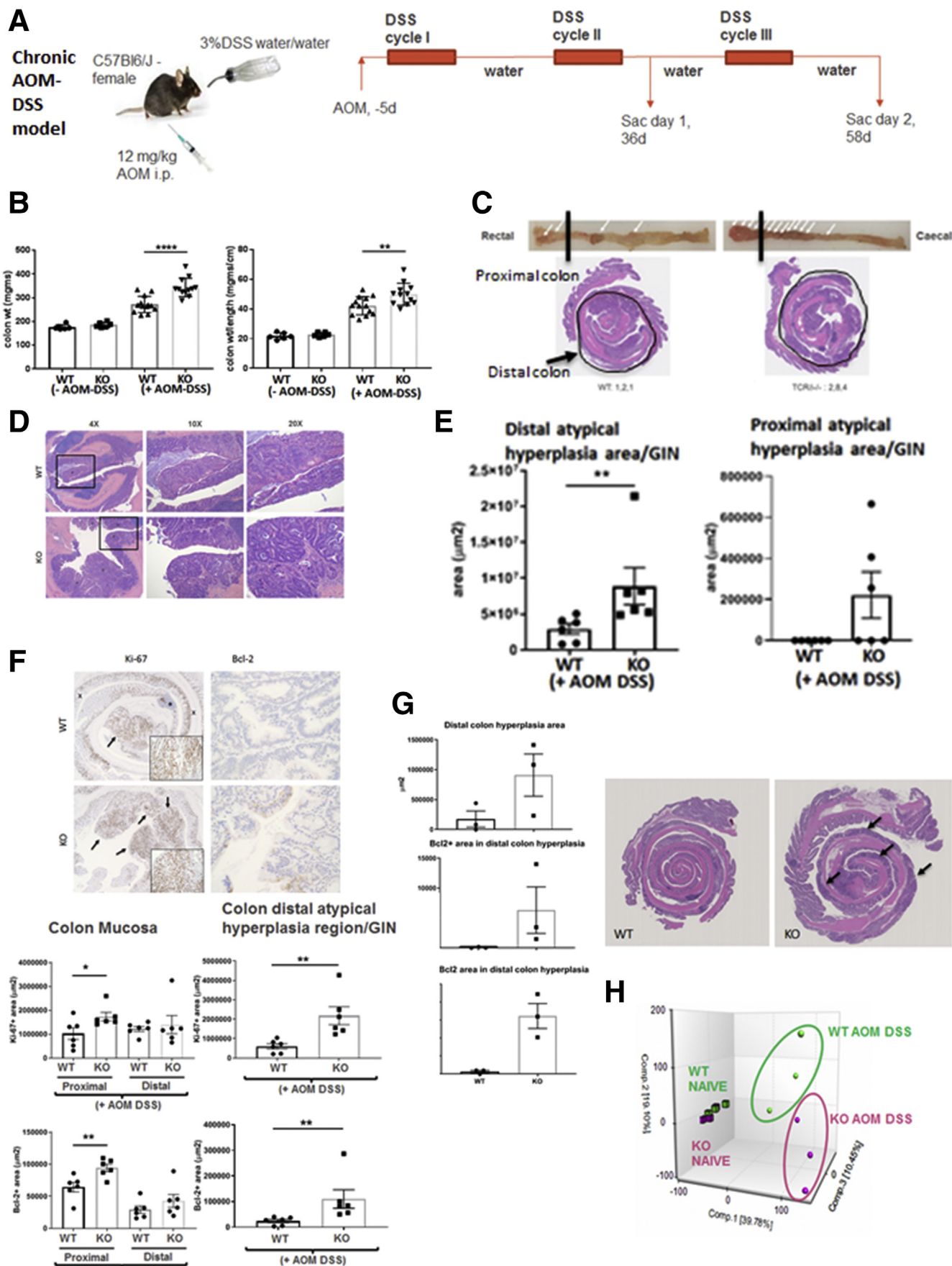
Supplementary Figure 2. (*See previous page*). **Pathology markers in AOM DSS model.** Experimental scheme of the chronic model showing treatment with AOM-DSS, and 2 time points of sacrifice: days 36 and day 58 (*A*). Day 58, colon weight and density (*B*), representative gross photographs showing polyps (*white arrows*, *upper panel*, *portion to the right of black bar* denoting region analyzed for histology) and subgross colon histology images (*lower panel*, *encircled region* denoting distal colon) (*C*). GIN (*asterisk*) in the distal colon 58 days after AOM-DSS treatment was limited to small regions in WT mice (*upper panel*) and was multifocal to widespread in TCRdKO mice (*lower panel*). The *boxes* in the *left panels* indicates the region highlighted in the *middle panels* (*D*). Comparative polyp (GIN) areas 58 days after AOM DSS treatment in the distal colon (*left panel*) and in the proximal colon (*right panel*) (*E*). Representative images of Ki67+ and Bcl2+ expression via IHC and quantification (*F*). (*G*) Comparative measurement of distal hyperplasia region (*top panel*) and Bcl-2+ area (*middle panel*) and % Bcl-2+ area in distal hyperplasia region (*bottom panel*) on day 36 colon. Polyps were not observed in the distal colon macroscopically at this time point, but were observed microscopically, as indicated by the *arrows* in the KO subgross image. (*H*) PCA showing the relative clustering of treatment groups. Error bars indicate mean $\pm$ SEM values for each *bar* and each *dot* represents an individual animal. Statistical analysis using nonparametric Mann-Whitney test was performed. **$P < .01$; *$P < .05$. GIN, Gastrointestinal intraepithelial neoplasia; IHC, immunohistochemistry; KO, knockout.
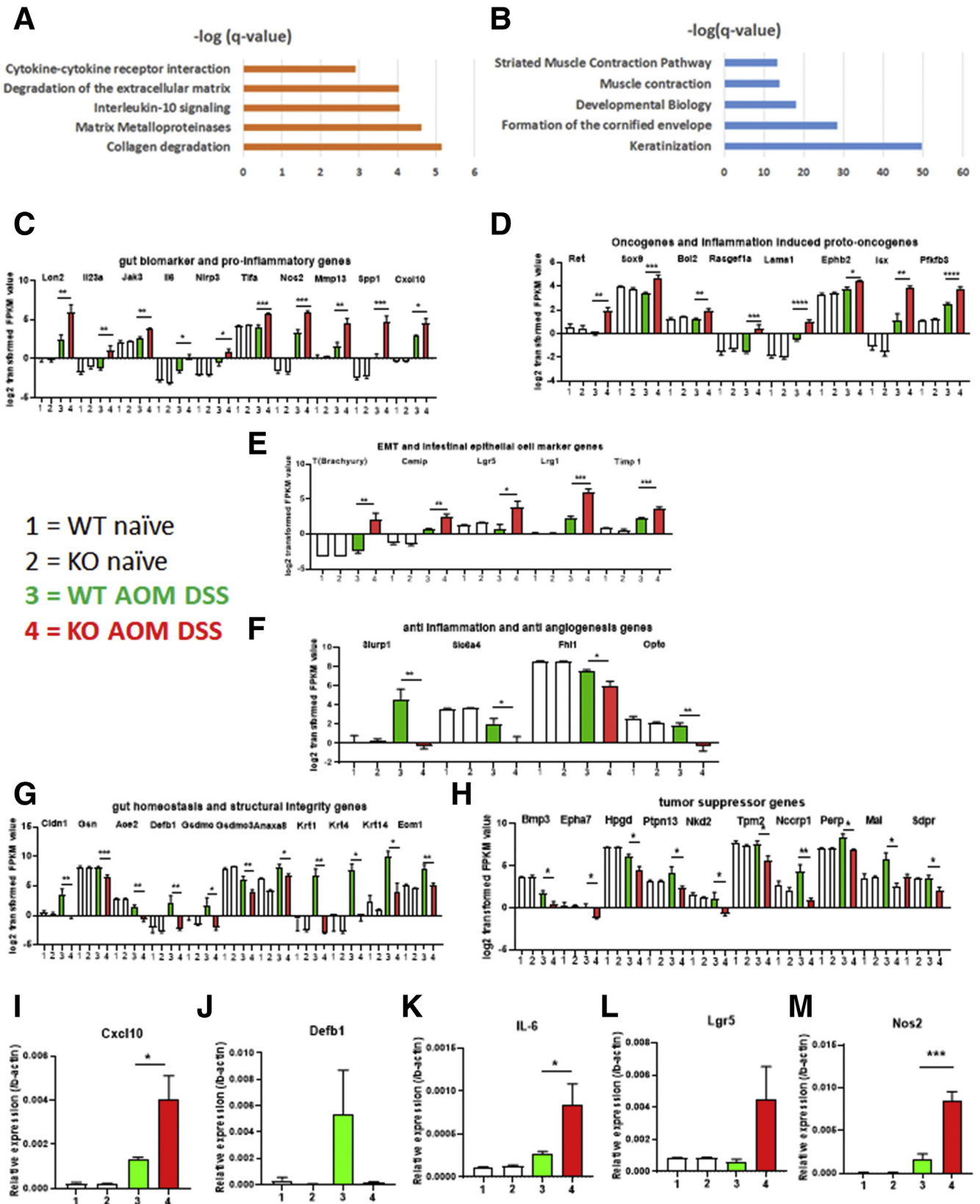
Supplementary Figure 3. (*See previous page*). **Transcriptomic changes in distal colon in early time point of AOM DSS model.** Bar chart representation of top 5 enriched pathways (CPDB) for both upregulated (*A*) and downregulated (*B*) DEGs between KO versus WT in AOM-DSS model. Selected upregulated biomarker and proinflammatory genes (*C*), oncogenes and inflammation-induced proto-oncogenes (*D*), epithelial mesenchymal transition (EMT) and gut epithelial stem cell marker genes (*E*) and selected downregulated anti-inflammatory and angiogenesis genes (*F*), gut homeostasis and structural integrity genes (*G*), and tumor suppressor genes (*H*). Selected upregulated and downregulated biomarker from bulk RNAseq validated by nanostring technology using inhouse predesigned inflammatory panel (*I-M*). Each gene is represented by 4 consecutive bar graphs representing WT naive (#1), KO naive (#2), WT AOM-DSS (#3), and KO AOM-DSS (#4), respectively. Statistical significance is only shown between the bar graphs #3 (*green*) and #4 (*red*) for each gene. Error bars signify mean $\pm$ SEM for each *bar* and each *dot* represent individual animal. Statistical analysis using 1-way analysis of variance with Tukey multiple comparison was performed using GraphPad Prism software. ****P < .0001; ***P < .001; **P < .01; *P < .05. KO, knockout.
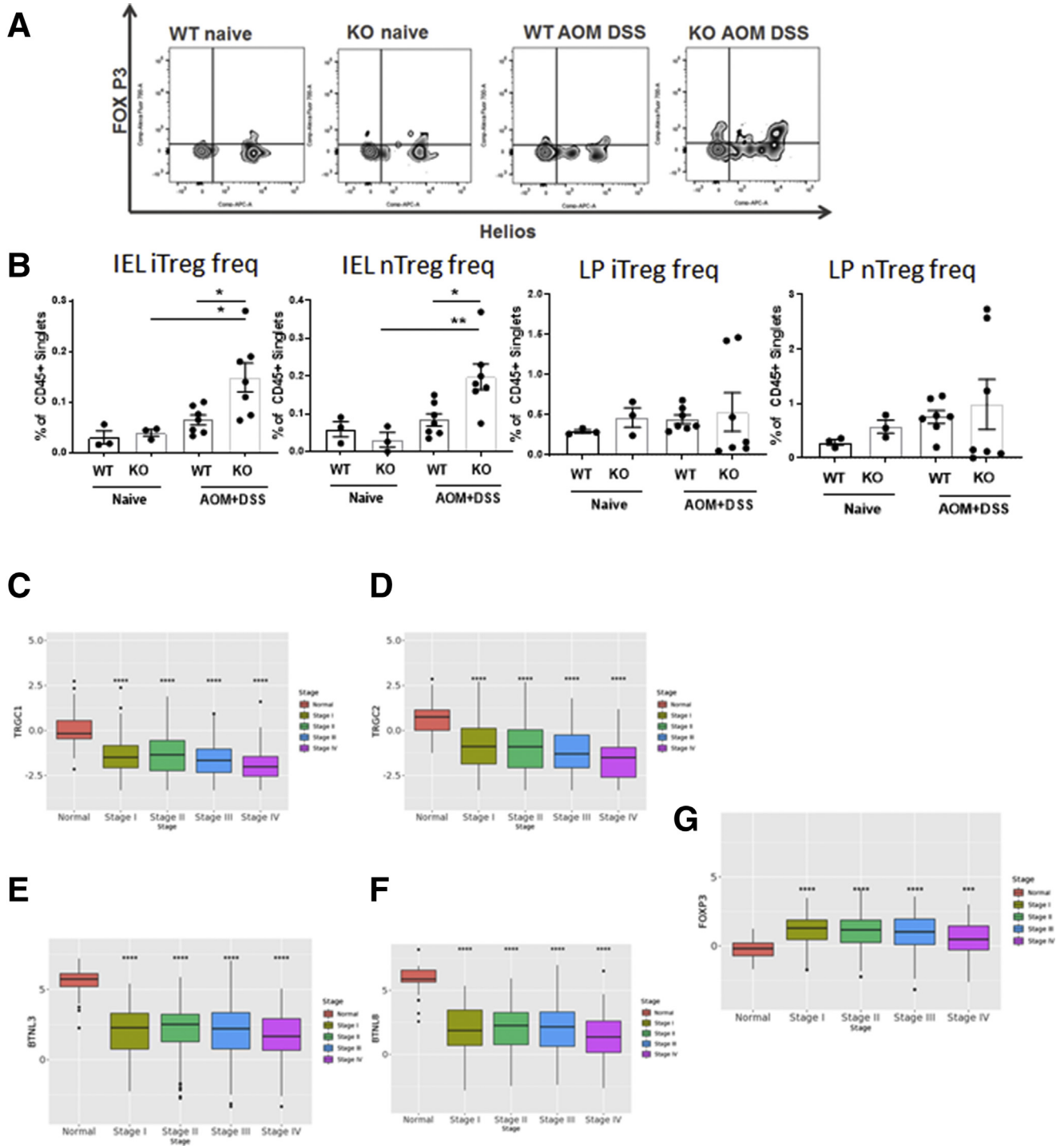
Supplementary Figure 4. Immunephenotype in murine and human colon. (*A*) Zebra plots for live, CD45+ Epcam- CD3+ GD- CD4+ gated events. FOX P3+ Helios- represents induced Tregs (iTregs) and FOX P3+ Helios+ represents natural Tregs (nTregs). (*B*) Bar graphs show comparative iTreg frequency (among live CD45+ Epcam- events) and nTreg frequency in IEL and LP fractions. Correlation of different genes of relevance in CRC patient datasets. Expression of TRGC (T-cell receptor gamma constant region genes, 1 and 2) at different stages of COAD tumors and related to normal (*C* and *D*). Expression of epithelial anchorage molecules BTNLs 3 and 8 known for human tissue resident γδ T cells (*E* and *F*). Positive correlation of important immunoregulatory molecule FOXP3 with different stages of COAD (*G*). IEL, intraepithelial lymphocytes.